BOR DERGİSİ
JOURNAL OF BORON
https://dergipark.org.tr/boron

The role of B_2O_3 in lithium-zinc-calcium-silicate glass for improving the radiation shielding competencies: A theoretical evaluation via Phy-X/PSD

Recep Kurtuluş[1], Taner Kavas[2*]

[1]Afyon Kocatepe University, Faculty of Engineering, Department of Materials Science and Engineering, Afyonkarahisar, 03200, Turkey, ORCID orcid.org/0000-0002-3206-9278
[2]Afyon Kocatepe University, Faculty of Engineering, Department of Materials Science and Engineering, Afyonkarahisar, 03200, Turkey, ORCID orcid.org/0000-0003-1070-8451

ARTICLE INFO

Article history:
Received December 16, 2020
Accepted January 28, 2021
Available online March 31, 2021

Research Article

DOI: 10.30728/boron.841726

Keywords:
B_2O_3
Glass
Gamma-rays
Phy-X/PSD
Radiation shielding

ABSTRACT

In this study, a preliminary theoretical investigation on lithium-zinc-calcium-silicate (LZCS) glass with a composition of *(15-x)*Li_2O*-10ZnO-10CaO-65*SiO_2*-x*B_2O_3 where *x: 0, 3, 6, 9, 12,* and *15 mol%* was performed to understand the effect of B_2O_3 on physical, optical, and radiation shielding properties. For this purpose, the L15B0 to L0B15 glass series was designed for evaluating glass density (ρ_{glass}), refractive index (n), mass attenuation coefficient (μ_m), and half-value layer ($\Delta_{0.5}$) parameters. The theoretical calculations showed that the increasing amount of B_2O_3 increased the overall ρ_{glass} from 2.9195 to 2.9865 g/cm^3. Further, the addition of B_2O_3 in substitution for Li_2O enhanced the n parameter from 1.6882 to 1.7626. Additionally, BatchMaker software aided to investigate viscosity behavior with the increasing temperature. We found out that the melting point of LZCS glass series ascends with the addition of B_2O_3, namely from 1309 to 1624 ºC. On the other hand, the newly developed Phy-X/PSD software computations paved the way for ascertaining μ_m and $\Delta_{0.5}$. According to the μ_m computations, one can clearly state that an increasing trend is observable against the increasing photon energy, but the L0B15 possessed an enhanced shielding ability than that of the remaining at all photon energies. Moreover, we found out that the $\Delta_{0.5}$ increased with respect to the ascending photon energies, however, the $\Delta_{0.5}$ was effectively improved with the addition of B_2O_3 in the order of L0B15<L3B12<L6B9<L9B6<L12B3<L15B0. Lastly, a comparison for $\Delta_{0.5}$ variations between L0B15 and commercially available RS253 G18 evidently demonstrated that L0B15 achieves 4.11 cm while RS253 G18 fulfills 4.95 which in turn confirms that the proposed glass system can be utilized in radiation shielding applications. All in all, B_2O_3 has promising effects on radiation shielding features in LZCS glass series.

1. Introduction

In today's world, the radiation term has become a major concern among the scientific community since artificial radiation sources have been exponentially increasing with the developing technological areas [1,2]. From medical diagnosis to industrial non-destructive tests, or from food sterilizations to communication systems the humanity has been facing with variety of irradiation including alpha, beta, gamma, or the like [3-5]. In fact, these rays have a strong probability of damage to human health with respect to time, exposure, and duration parameters. DNA mutations, skin burns, or even cancer problems may raise as a result of exposure to these irradiations [6,7]. From this point of view, the usage of a radiation shielding material against incoming rays has become a major action in order to be protected from the above-mentioned health risks. Radiation shielding material can, therefore, minimize the incoming photon energy thanks to the attenuation characteristics they have, and thus workers and/or patients can be safeguarded [8].

Conceptually, attenuation of incoming photon energy is directly associated with the atomic mass, atomic radius, and density value of the substance used. This is because higher molecular mass or higher atomic radius can contribute enhacing the attenuation competencies of the radiation shielding material, which in turn facilitating the interaction between incoming rays and materials. Within the scope of practically preferred radiation shielding materials, metallic lead finds a broad application area due to its appreciable density value (11.32 g/cm^3) [9,10]. The rooms where these devices with the capability of irradiations are placed have been covered with the use of metallic lead in accordance

*Corresponding author: tkavas@aku.edu.tr

with the regulations. Despite the great benefits of metallic lead in terms of advanced attenuating characteristics in particular to the higher photon energies (i.e. gamma-rays), the toxicity issue on humans and the environment has recently begun to be restricted its wide preference [11]. An alternative material, heavy-weight concrete containing aggregates, has become of interest because the building blocks can be fabricated by considering the possible effects of photon energies [12,13]. In fact, heavy-weight aggregates such as barite can be inserted in concrete blends for improving radiation shielding features [14]. Nevertheless, the cracking problem during operation is the primary deficiency of heavy-weight concrete materials. Even though the mentioned problems are valid for these shielding materials the employment has still in progress due to the lack of alternative materials. That's why scientists have extensively been continuing to search for more options.

Glass materials offer spectacular features in many different applications including from daily needs to advanced optical fibers. One of the most essential properties of glass materials is the transparent appearance which metallic lead and heavy-weight concrete could not have. Additionally, compositional flexibility, being environmentally-friendly, well-known melting and shaping techniques, as well as relatively lower production costs make glass materials preferable in radiation shielding applications [15]. Commercially, there are diverse glass types involving silicates, borates, phosphates, and so on. Among these, lithium-zinc-silicate (LZS) glass is regarded as an essential system for various applications such as sealing, dental, and dielectrics. This is because, wide thermal expansion range (5 to 20x10^{-6} $^{o}C^{-1}$), ability for glass-ceramic formations, relatively good glass viscosity behavior, high electrical insulation, and considerable density values can be obtained with the use of LZS glasses which in turn possessing great potential for radiation shielding applications [16,17]. Furthermore, calcium oxide (CaO) which has a relatively high density value (3.34 g/cm^3) can aid to improve radiation shielding characteristics in the LZS glass system since its positive effect on different glass system has been confirmed by numerous literature studies [18,19]. On the other hand, boron oxide (B_2O_3) can ensure a lot of benefits including low thermal expansion coefficient, facilitating melting conditions, increasing chemical durability, and good glass formation ability [20]. From the perspectives of radiation shielding features, B_2O_3 presents superior shielding abilities, particularly against neutron scatterings. Additionally, Turkey is the leading country in terms of boron reserves, and hence value-added applications involving boron compounds can bring countless benefits both economically and strategically [21, 22]. In conclusion for the selection of LZS glass system and B_2O_3 content, it is worth to investigate the role of B_2O_3 in the LZS glass systems for enhancing radiation shielding competencies.

Literature is generally focused on the understanding the characteristics of LZS glass system with respect to physical, chemical, mechanical, and thermal properties. However, it is evident that the radiation shielding competencies is lack of investigation, in this regard. From the perspective of lithium-zinc-added glass systems, we come forward numerous studies on radiation shielding properties [23-25]. Moreover, silicate-based glass systems are of interest by many researchers for doping and adding various oxide contents [26-28]. As can be appreciated from the literature works, no further investigations have been made on LZS or LZCS glass systems. Indeed, the role of B_2O_3 in the LZCS glass system has not been experiences both theoretically and experimentally. Therefore, the authors strongly believe that any findings will make difference in the literature for further explorations.

In the present study, a lithium-zinc-calcium-silicate (LZCS) glass system reinforced with B_2O_3 was examined with the use of Phy-X/PSD software. For this, the dopant was designed in the glass system of *(15-x)* Li_2O-*10ZnO-10CaO-65*SiO_2-*x*B_2O_3 where *x: 0, 3, 6, 9, 12*, and *15 mol%* to obtain the L15B0 to L0B15 glass series. Glass density (ρ_{glass}) and refractive index (*n*) calculations were conducted to determine the possible alterations. Furthermore, viscosity versus temperature profiles was drawn with the use of BatchMaker software for understanding glass melting characteristics. Lastly, a comparison between the LZCS series and commercial radiation shielding materials were done to make a deeper sense for our study. As a result, this study reported the new results on LZCS containing B_2O_3 glass system which has not previously been investigated in the literature studies.

2. Materials and Methods

2.1. Compositional Design

To understand the role of B_2O_3 in LZCS glass system, we designed a distinct composition series as listed in Table 1. L15B0 represents the oxide content with molar percentage for lithium oxide and boron oxide as 15 and 0 mol%, respectively. The remainings are also signified with respect to these codes.

Table 1. The compositional design for LZCS glass system in mol%.

Code	Li_2O	ZnO	CaO	SiO_2	B_2O_3
L15B0	15,00	10,00	10,00	65,00	0,00
L12B3	12,00	10,00	10,00	65,00	3,00
L9B6	9,00	10,00	10,00	65,00	6,00
L6B9	6,00	10,00	10,00	65,00	9,00
L3B12	3,00	10,00	10,00	65,00	12,00
L0B15	0,00	10,00	10,00	65,00	15,00

2.2. Calculations for Physical and Optical Properties

Glass density (ρ_{glass}) parameter plays an essential characteristics on the investigated glass systems. To find out the changes in ρ_{glass} with the insertion of B_2O_3 in LZCS glass system, it is beneficial to apply emprical relation stated by Inaba and Fujino [29] as expressed in Equation 1. Here, M_i, V_i and x_i indicate molecular weight (g/mol), packing density factor (cm^3/mol), and molar fraction of i^{th} component, respectively.

$$\rho = (0{,}53).\frac{(\sum M_i.x_i)}{(\sum V_i.x_i)} \quad (1)$$

Another essential parameter, refractive index (n), is the key factor determining optical properties of glass materials. To calculate this parameter, energy band gap (E_g) values of each oxide is employed throughout the Equation 2 [30].

$$\frac{n^2-1}{n^2+2} = 1 - \sqrt{\frac{E_g}{20}} \quad (2)$$

2.3. Glass Viscosity Behavior

Estimating the glass viscosity behavior with respect to temperature changes takes great importance before experimental studies. In literature, there are few works focusing on viscosity alterations for glass systems in the perspective of computational aspects. For this reason, BatchMaker software which utilizes numerous property calculations based on glass oxide contents emerges as an efficient tool for determining viscosity versus temperature profiles [31]. The software takes into consideration the findings of Lakatos et al. [32] and Fluegel [33] in this respect. We employed a calculation set up for our LZCS glass series, and drawed viscosity versus temperature profiles to make a deeper understanding on B_2O_3 insertion in substitution for Li_2O.

2.4. Radiation Shielding Computations

Owing to the newly developed user-friendly software, Phy-X/PSD, the radiation shielding parameters can be computed in an efficient way. Within the scope of Phy-X/PSD, one can simply input glass composition and the related glass density to the software. After this, the software begins for computing the variables for figuring out the different radiation shielding parameters [19]. Here, we evaluated some essential parameters including mass attenuation coefficient (μ_m) and half-value layer ($\Delta_{0.5}$). As is known, the μ_m defines the interaction between incoming ray and the matter of unit mass per unit region whereas $\Delta_{0.5}$ indicates the thickness where the energy of incoming photon is attenuated to its half value. Equations 3 and 4 were used aid to calculate the parameters.

$$\mu_m = \frac{\mu}{\rho_{glass}} \quad (3)$$

where μ is the linear attenuation coefficient, and ρ_{glass} is the overall glass density for each samples.

$$\Delta_{0.5} = \frac{ln2}{\mu} \quad (4)$$

3. Results and Discussion

3.1. Physical and Optical Properties

In literature, almost all researchers have identified the one of the most important parameter, glass density (ρ_{glass}). This is because radiation shielding competencies are straight-forwardly associated with the ρ_{glass} value. As a general concept, it is expected to have higher ρ_{glass} value as possible for enhancing the radiation shielding features [34,35]. From this point of view, the authors calculated the theoretical ρglass values for the examined glass series. On the other hand, refractive index (n) is a measure of the interaction between incident ray and the matter. The incident ray may be encountered with refraction, absorption, or transmission with respect to the interaction phenomenon. We know that the higher the n value for the glass system the more efficient the radiation shielding will [36]. For understanding the possible alteration in n value for our glass systems, we evaluated the theoretical n calculations for each glass samples. Furthermore, since both ρ_{glass} and n parameters have a parallel behavior Figure 1 depicts the changes in these properties with regard to the B_2O_3 addition. One can firmly deduce that both parameters are in increasing trend with the increasing insertion ratio of B_2O_3. For instance, L15B0 sample has a ρ_{glass} value of 2.9195 g/cm^3 whereas L0B15 sample gains 2.9865 g/cm^3. This situation may be attributed to the higher molecular mass of B_2O_3 (69.62

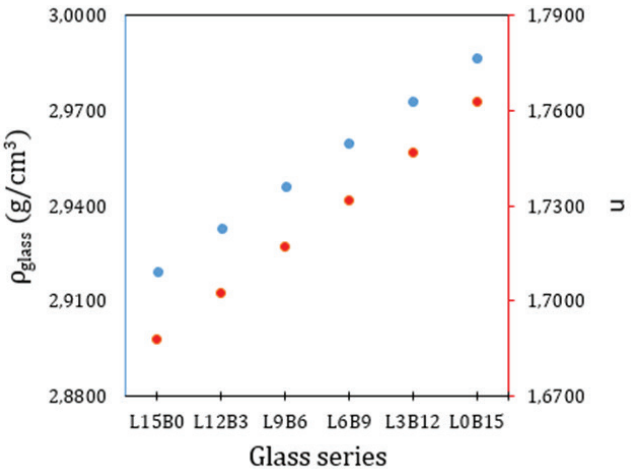

Figure 1. Alteration of ρglass (blue dots) and n (red dots) with respect to the B_2O_3 addition for the investigated LZCS glass series.

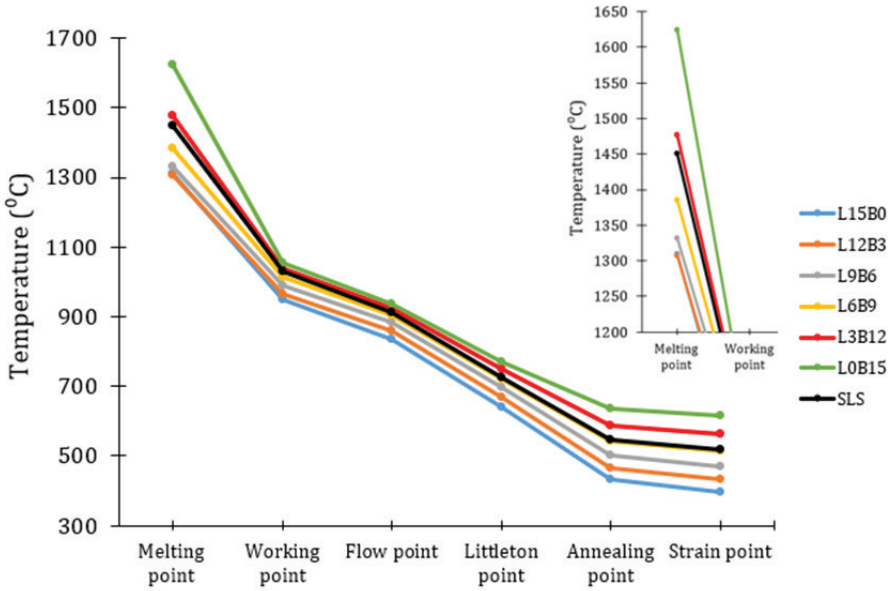

Figure 2. Viscosity versus temperature profiles for the investigated LZCS glass series.

g/mol) in comparison to Li_2O (29.88 g/mol). Similar findings were also stated with some literature studies conducted by [37,38]. On the other hand, the contribution of B_2O_3 in place of Li_2O enhance the *n* parameter in the order of L0B15>L3B12>L6B9>L9B6>L12B3>L 15BO. This is because the E_g value for B_2O_3-added series are becoming lower, and thus the incident rays could not transmitted throughtout the glass substance. In other words, much more incoming photon energy becomes interacted with the glass substance, particularly, herein, boron atoms. Therefore, the insertion of B_2O_3 possesses successful conclusions on both parameters.

3.2. Viscosity versus Temperature Profiles

The investigated LZCS glass series are evaluated in terms of viscosity behaviour with respect to the varying temperature via using BatchMaker software in Figure 2. For making a sensible comments on the behavior of the LZCS series, a well-known glass type as soda-lime-silica (SLS) is also depicted. From the profiles, it is obvious that the increasing amount of B_2O_3 has an adverse effect on melting temperature. To exemplify, L15B0 specimen has a value of 1309ºC for melting point whereas L0B15 acquires 1624ºC. At this point, SLS glass possesses nearly 1450ºC as a melting point. The reason behind this phenomenon may be referred to the glass-forming characteristics of B_2O_3 rather than fluxing agent behavior of Li_2O. The decrease in the amount of fluxing agent in the LZCS glass system ascends the liquidus point through lack of sufficient liquid phase. Therefore, we can report that the insertion of B_2O_3 in substitution for Li_2O in the LZCS glass system elevates the glass melting point.

3.3. Radiation Shielding Features

For highlighting the radiation shielding features of the examined LZCS glass series, we evaluated the most essential parameters as μ_m and $\Delta_{0.5}$. Figure 3 displays the mass attenuation coefficients (μ_m) with respect to incoming photon energies. It can be observed that the μ_m is found to be in increasing trend as a function of the increasing photon energy. In the lower photon energy levels, *i.e.* <0.015 MeV, the μ_m values range around 15 cm^2/g. However, a sudden decrease can be observable towards the increasing photon energy, *i.e.* 0.1 MeV. In this case, the μ_m descends through 0.20 cm^2/g. For the higher photon energies, *i.e.* >1 MeV, we gain the μ_m around 0.02 cm^2/g. Such a behavior may be attributed to the well-known three mechanisms as photoelectric absorption at low energy, Compton scattering at intermediate energy, and pair production process at high energy. On the other hand, when it comes to evaluate the effect of B_2O_3 in replacement for Li_2O, it is apperant that the B_2O_3 is directly enhancing the μ_m values at all photon energy levels. The μ_m is increased from 0.628 to 0.631 cm^2/g with the insertion ratio of B_2O_3 from 0 to 15 mol% at 1.30 MeV. This

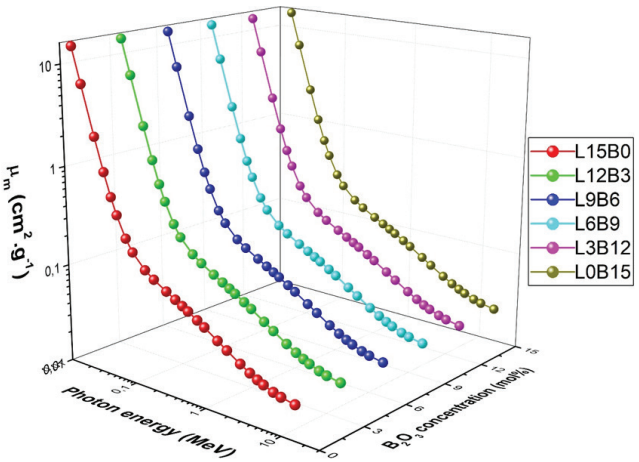

Figure 3. Mass attenuation coefficient of LZCS glass series with respect to photon energies.

increase is associateed with the higher density value of B_2O_3 (2.46 g/cm^3) than that of Li_2O (2.01 g/cm^3). The higher the glass density the better the radiation shielding competencies were confirmed by various studies in the literature [39,40]. Since an increasing trend is required for improving radiation shielding competencies we can report that B_2O_3 can provide this enhancement in an efficient way.

Yet another significant parameter, half-value layer ($\Delta_{0.5}$), signifies the required thickness value to attenuate the half of incoming energy. From this perspetive, Figure 4 reveals the variations in $\Delta_{0.5}$ for different photon energies. It is clear that the required thickness value for all LZCS glass series ascends with the increasing photon energy. However, L0B15 dominates over the remaining in all photon energies. For instance, L15B0 requires the $\Delta_{0.5}$ value of 3.39 cm while L0B15 yields 3.30 cm. That means the lesser thickness can attenuate the half of the incoming energy owing to the contribution of B_2O_3. In fact, the higher molecular mass of B_2O_3 (69.62 g/mol) compared to Li_2O (29.88 g/mol) is the reason facilitating this advancement. Moreover, a comparison between L0B15 and commercial radiation shielding glasses (*i.e.* Schott RS series) can make a better understanding of the figured out $\Delta_{0.5}$ values. Schott RS series have distinct type of glasses for the required photon energies [41]. Here, it may be more plausible to highlight the higher energy levels such as gamma-rays occurred at 1.25 MeV (^{60}Co). Besides, it may be more meaningful to select the lead-free RS series such as RS 253 G18 since our LZCS glass series do not contain any lead oxide substance. When it comes to compare $\Delta_{0.5}$ values, L0B15 specimen provides 4.11 cm while RS 253 G18 ensures 4.95 cm. From these values, we can firmly report that L0B15 sample achieves better radiation shielding features than that of commercially available RS 253 G15 glass. Therefore, our glass system can make a difference in a commercial manner.

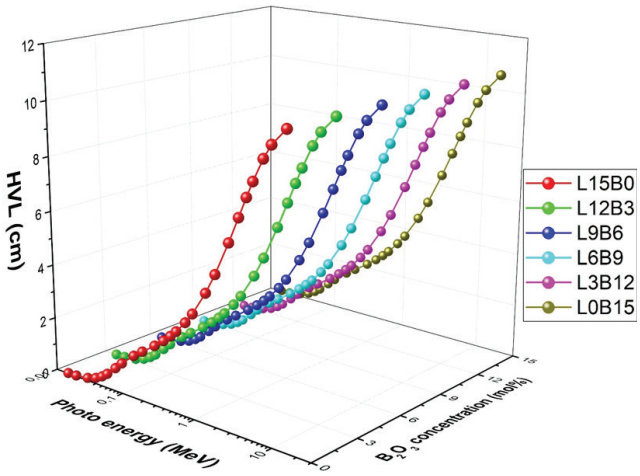

Figure 4. Half-value layer alterations with respec to photon energies for the LZCS series.

4. Conclusions

The present study focused on the theoretical calculations for evaluating the effects of B_2O_3 addition on the physical, optical, and radiation shielding properties of the lithium-zinc-calcium-silicate (LZCS) glass system. For this, *(15-x)Li_2O-10ZnO-10CaO-65SiO_2-xB_2O_3* where *x: 0, 3, 6, 9, 12,* and *15 mol%* glass system was designed, and L15B0 to L0B15 glass series were examined. The glass density (ρ_{glass}) calculations presented that B_2O_3 insertion is an efficient way to increase the overall ρglass. Additionally, the refractive index (n) value was enhanced owing to the B_2O_3 contribution. For understanding the viscosity behavior of the investigated glass series, BatchMaker software was utilized. It showed that the addition of B_2O_3 increased the melting point of the glass series due to the glass-forming role. In the perspective of radiation shielding features, the newly developed Phy-X/PSD software provided to compute mass attenuation coefficient (μ_m) and half-value layer ($\Delta_{0.5}$). We found out that the increasing content of B_2O_3 increased the μ_m and decreased the $\Delta_{0.5}$. These alterations ensured to improve radiation shielding characteristics for B_2O_3-reinforced LZCS series. More essentially, the L0B15 sample can compete with the commercial radiation shielding glass, particularly the lead-free series of RS 263 G18. In conclusion, the authors reported that the insertion of B_2O_3 is a good candidate for the LZCS glass system for the obtainment of advanced physical, optical, and radiation shielding features in comparison to the undoped situation.

References

[1] Gökmen, U., Özkan, Z., Jamalgolzari, L. E., & Ocak, S. B. (2020). Investigation of radiation attenuation properties of Al-Cu matrix composites reinforced by different amount of B4C particles. *Journal of Boron*, *5*(3), 124-130.

[2] Rammah, Y. S., Olarinoye, I. O., El-Agawany, F. I., & El-Adawy, A. (2020). Environment friendly La3+ ions doped phosphate glasses/glass-ceramics for gamma radiation shielding: Their potential in nuclear safety applications. *Ceramics International*, *46*(17), 27616-27626.

[3] Bektasoglu, M., & Mohammad, M. A. (2020). Investigation of radiation shielding properties of TeO2-ZnO-Nb2O5-Gd2O3 glasses at medical diagnostic energies. *Ceramics International*, *46*(10), 16217-16223.

[4] Jawad, A. A., Demirkol, N., Gunoğlu, K., & Akkurt, I. (2019). Radiation shielding properties of some ceramic wasted samples. *International Journal of Environmental Science and Technology*, *16*(9), 5039-5042.

[5] Saddeek, Y. B., Issa, S. A., Guclu, E. A., Kilicoglu, O., Susoy, G., & Tekin, H. O. (2020). Alkaline phosphate glasses and synergistic impact of germanium oxide (GeO2) additive: mechanical and nuclear radiation shielding behaviors. *Ceramics International*, *46*(10), 16781-16797.

[6] Gaikwad, D. K., Sayyed, M. I., Botewad, S. N., Obaid,

S. S., Khattari, Z. Y., Gawai, U. P., ... & Pawar, P. P. (2019). Physical, structural, optical investigation and shielding features of tungsten bismuth tellurite based glasses. *Journal of Non-Crystalline Solids*, *503*, 158-168.

[7] Aly, P., El-Kheshen, A. A., Abou-Gabal, H., & Agamy, S. (2020). Structural investigation and measurement of the shielding effect of borosilicate glass containing PbO, SrO, and BaO against gamma irradiation. *Journal of Physics and Chemistry of Solids*, *145*, 109521.

[8] Vighnesh, K. R., Ramya, B., Nimitha, S., Wagh, A., Sayyed, M. I., Sakar, E., ... & Kamath, S. D. (2020). Structural, optical, thermal, mechanical, morphological & radiation shielding parameters of Pr3+ doped ZAlFB glass systems. *Optical Materials*, *99*, 109512.

[9] Al-Hadeethi, Y., & Sayyed, M. I. (2019). Analysis of borosilicate glasses doped with heavy metal oxides for gamma radiation shielding application using Geant4 simulation code. *Ceramics International*, *45*(18), 24858-24864.

[10] Mirji, R., & Lobo, B. (2017). 24. Radiation shielding materials: A brief review on methods, scope and significance. *In National Conference on 'Advances in VLSI and Microelectronics.'In PC Jabin Science College, Huballi, India* (pp. 96-100).

[11] Ara, A., & Usmani, J. A. (2015). Lead toxicity: a review. *Interdisciplinary Toxicology*, *8*(2), 55-64.

[12] Demir, F., Budak, G., Sahin, R., Karabulut, A., Oltulu, M., Şerifoğlu, K., & Un, A. (2010). Radiation transmission of heavyweight and normal-weight concretes containing colemanite for 6 MV and 18 MV X-rays using linear accelerator. *Annals of Nuclear Energy*, *37*(3), 339-344.

[13] Maslehuddin, M., Naqvi, A. A., Ibrahim, M., & Kalakada, Z. (2013). Radiation shielding properties of concrete with electric arc furnace slag aggregates and steel shots. *Annals of Nuclear Energy*, *53*, 192-196.

[14] Saidani, K., Ajam, L., & Ouezdou, M. B. (2015). Barite powder as sand substitution in concrete: Effect on some mechanical properties. Construction and Building Materials, *95*, 287-295.

[15] Kurtulus, R., & Kavas, T. (2020). Investigation on the physical properties, shielding parameters, glass formation ability, and cost analysis for waste soda-lime-silica (SLS) glass containing SrO. *Radiation Physics and Chemistry*, *176*, 109090.

[16] Shen, Z., Zhu, L., Zhang, Y., Chen, Y., Yang, D., & Song, X. (2017). Effect of CuO addition on crystallization and thermal expansion properties of Li2O-ZnO-SiO2 glass-ceramics. *Ceramics International*, *43*(9), 7099-7105.

[17] Goswami, M., Deshpande, S. K., Kumar, R., & Kothiyal, G. P. (2010). Electrical behaviour of Li2O-ZnO-SiO2 glass and glass-ceramics system. *Journal of Physics and Chemistry of Solids*, *71*(5), 739-744.

[18] Al-Hadeethi, Y., Sayyed, M. I., & Rammah, Y. S. (2019). Investigations of the physical, structural, optical and gamma-rays shielding features of B2O3-Bi2O3-ZnO-CaO glasses. *Ceramics International*, *45*(16), 20724-20732.

[19] Singh, K., Singh, H., Sharma, G., Gerward, L., Khanna, A., Kumar, R., ... & Sahota, H. S. (2005). Gamma-ray shielding properties of CaO-SrO-B2O3 glasses. *Radiation Physics and Chemistry*, *72*(2-3), 225-228.

[20] Abouhaswa, A. S., & Kavaz, E. (2020). A novel B2O3-Na2O-BaO-HgO glass system: Synthesis, physical, optical and nuclear shielding features. *Ceramics International*, *46*(10), 16166-16177.

[21] *Boron in the world*. (2020). Etimaden. Retrieved December 15, 2020 from https://www.etimaden.gov.tr/en/boron-in-the-world.

[22] *Reserves*. (2018). TENMAK BOREN. Retrieved December 15, 2020 from https://www.boren.gov.tr/Sayfa/reserves/103.

[23] Yalcin, S., Aktas, B., & Yilmaz, D. (2019). Radiation shielding properties of Cerium oxide and erbium oxide doped obsidian glass. *Radiation Physics and Chemistry*, *160*, 83-88.

[24] Sayyed, M. I., Lakshminarayana, G., Moghaddasi, M., Kityk, I. V., & Mahdi, M. A. (2018). Physical properties, optical band gaps and radiation shielding parameters exploration for Dy3+-doped alkali/mixed alkali multicomponent borate glasses. *Glass Physics and Chemistry*, *44*(4), 279-291.

[25] Rashad, M., Ali, A. M., Sayyed, M. I., Somaily, H. H., Algarni, H., & Rammah, Y. S. (2020). Radiation attenuation and optical features of lithium borate glasses containing barium: B2O3·Li2O·BaO. *Ceramics International*, *46*(13), 21000-21007.

[26] Khodadadi, A., & Taherian, R. (2020). Investigation on the radiation shielding properties of lead silicate glasses modified by ZnO and BaO. *Materials Chemistry and Physics*, *251*, 123136.

[27] Çetin, B., Yalçin, Ş., & Albaşkara, M. (2017). Investigation of radiation shielding properties of soda-lime-silica glasses doped with different food materials. *Acta Physica Polonica*, A., *132*(3), 988-990.

[28] Sayyed, M. I., Elmahroug, Y., Elbashir, B. O., & Issa, S. A. (2017). Gamma-ray shielding properties of zinc oxide soda lime silica glasses. *Journal of Materials Science: Materials in Electronics*, *28*(5), 4064-4074.

[29] Inaba, S., & Fujino, S. (2010). Empirical equation for calculating the density of oxide glasses. *Journal of the American Ceramic Society*, *93*(1), 217-220.

[30] Thombare, M., Joat, R., THombre, D., & Mahavidyalaya, V. B. (2016). Glasses study physical properties of sodiumborophosphate. *International Journal of Engineering Science*, 8482.

[31] *BatchMaker® Batch Calculation & Glass Development.* (2020). ilis GmbH. Retrieved December 15, 2020 from https://www.ilis.de/en/batchmaker.html.

[32] Lakatos, C. Johansson, L. G., & Simmingskold, B. (1972). Viscosity temperature relations in the glass system SiO2-Al2O3-Na2O-K2O-CaO-MgO in the composition range of technical glasses. *Glass Technology-European Journal of Glass Science and Technology Part A*, *13*(3), 88-95.

[33] Fluegel, A. (2007). Glass viscosity calculation based on a global statistical modelling approach. *Glass Technology-European Journal of Glass Science and Technology Part A*, *48*(1), 13-30.

[34] Al-Hadeethi, Y., & Sayyed, M. I. (2020). A comprehensive study on the effect of TeO2 on the radiation shielding properties of TeO2-B2O3-Bi2O3-LiF-SrCl2 glass system using Phy-X/PSD software. *Ceramics In-*

ternational, *46*(5), 6136-6140.

[35] Al-Hadeethi, Y., Sayyed, M. I., Kaewkhao, J., Askin, A., Raffah, B. M., Mkawi, E. M., & Rajaramakrishna, R. (2019). Physical, structural, optical, and radiation shielding properties of B2O3-Gd2O3-Y2O3 glass system. *Applied Physics A*, *125*(12), 1-7.

[36] Wahab, E. A., Shaaban, K. S., & Elsaman, R. (2019). Radiation shielding and physical properties of lead borate glass-doped ZrO2 nanoparticles. *Applied Physics A*, *125*(12), 1-15.

[37] Susoy, G. (2020). Effect of TeO2 additions on nuclear radiation shielding behavior of Li2O-B2O3-P2O5-TeO2 glass-system. *Ceramics International*, *46*(3), 3844-3854.

[38] Kumar, A. (2017). Gamma ray shielding properties of PbO-Li2O-B2O3 glasses. *Radiation Physics and Chemistry*, *136*, 50-53.

[39] Lakshminarayana, G., Elmahroug, Y., Kumar, A., Dong, M. G., Lee, D. E., Yoon, J., & Park, T. (2020). TeO2-B2O3-ZnO-La2O3 glasses: γ-ray and neutron attenuation characteristics analysis by WinXCOM program, MCNP5, Geant4, and Penelope simulation codes. *Ceramics International*, *46*(10), 16620-16635.

[40] Al-Hadeethi, Y., Sayyed, M. I., Mohammed, H., & Rimondini, L. (2020). X-ray photons attenuation characteristics for two tellurite based glass systems at dental diagnostic energies. *Ceramics International*, *46*(1), 251-257.

[41] Radiation Shielding Glasses for Industrial Applications. (2020). Schott AG. Retrieved December 15, 2020 from https://www.schott.com/advanced_optics/english/products/optical-materials/specialmaterials/radiation-shielding-glasses/index.html.